AIAA 80-1278R

Bond Stress Transducer Design for Solid Propellant Rocket Motors

E.C. Francis* and R.E. Thompson†
United Technologies Corporation, Sunnyvale, Calif.

An improved miniature pressure transducer has been developed for use in measuring stress in solid grain rocket motors. The requirements for survival and performance are such that the sensor has direct use as a general pressure transducer especially where small size and high reliability are a requirement. This paper summarizes the design work and presents some long-term performance results as well as other test data. Design of this reliable stress transducer for embedment in a solid propellant rocket motor has utilized finite-element structural analysis to reduce the stress disturbance above the external transducer body and to optimize diaphragm interaction with the nonlinear viscoelastic solid propellant. Minimizing the interaction between solid propellant and transducer diaphragm required that the transducer body and flexural diaphragm be much stiffer than conventional pressure transducers.

Introduction

MODIFIED pressure transducers have previously been used to measure the normal bond stresses between the solid propellant and the rocket motor case. Accuracy and stability of the early units were poor since periodic measurements taken in either laboratory or motor applications could not be repeated.

Early diaphragm-type transducers experienced the following two major problems:

1) Mechanical and electrical stability of the transducers were poor because of inadequate transducer structural design and fabrication procedures.[1] Also, there was insufficient chemical protection for the electrical components from the corrosive propellant environment.[2]

2) The disturbance of the propellant stress field in the neighborhood of the embedded stress transducer was poorly understood and the sensing diaphragm-to-propellant interaction was not minimized to avoid nonlinear diaphragm performance. Older style transducers were optimized for large electrical output rather than diaphragm stiffness.

The first problem was solved by designing the transducer for chemical protection and specifying fabrication materials and fabrication procedures that would minimize epoxy creep, metal instability after machining, and long-time drift of components.

The second problem was minimized by optimizing the transducer internal and external design to reduce the transducer-propellant disturbance and interaction.[3] The final transducer, which is detailed later in this paper, is manufactured from 15-5 SS which has undergone a special heat treatment to minimize the thermally induced stresses. The semiconductor strain gages are bonded to the inside of the diaphragm and are completely protected from the corrosive propellant environment as are the lead wires which are inside a flexible tube. Very stable temperature compensation and bridge completion resistors are located remotely at the end of the lead wire tube in a metal housing protecting them from the environment.

Presented as Paper 80-1278 at the AIAA/SAE/ASME 16th Joint Propulsion Conference, Hartford, Conn., June 30-July 2, 1980; submitted Aug. 25, 1980: revision received April 7, 1981.

*Chief, Structural Research, R&AT Department, Chemical Systems Division.

†Manager, Structural Research Laboratory, Chemical Systems Division.

Design Trade-Off

This section of the report presents some engineering considerations in the transducer design. As is the case with most design work, various engineering trade-off decisions were required. The order of importance has been described in the introduction.

Various multimaterial, electrical and mechanical properties interact and each affects one or more performance parameters in varying degrees. Areas of concern are:

1) Diaphragm strain distribution on the semiconductor strain gages and metal stability factors.

2) Epoxy shear stress distribution and stability factors.

3) Semiconductor strain gage transfer strain and stability factors.

4) Relative thermal expansions between diaphragm, gage, and epoxy.

5) Electrical characteristics of the semiconductor strain gage.

6) Temperature compensation techniques.

Each of the above have been studied. For the sake of brevity, only the most important are presented herein.

Metal Stability

The stress-strain curve shown in Fig. 1 illustrates typical metal structural behavior. When applied stresses exceed the linear range of behavior, the material will not return to its original condition. The metal could have a 2000 microstrain offset by the material's elastic limit definition. This is adequate for most structural applications where long-time stability and accuracy are not important. For the stress transducer with a maximum loaded diaphragm strain of 100 microstrain, a 2000-microstrain offset is many times greater than full-scale strain of the transducer. For this reason care must be taken to avoid the metal offset problem caused by high stress conditions.

The precision elastic limit, PEL, defines a metal offset of only 1 microstrain (Fig. 1). The PEL is usually much less than the proportional elastic limit. The PEL data are generally obtained by slow cyclic loadings in incremental steps (Fig. 2) until a 1-microstrain offset is achieved in the metal. Creep of the transducer metal diaphragm over many years would produce electrical offsets which could erroneously be interpreted as a propellant stress change. Typical creep curves for 310 stainless steel at different temperatures are shown in Figs. 3 and 4 to illustrate the degree of microcreep phenomenon that occurs. The creep strains are much greater than full-scale output strains for the current transducer application. It is very important to stay well below the PEL

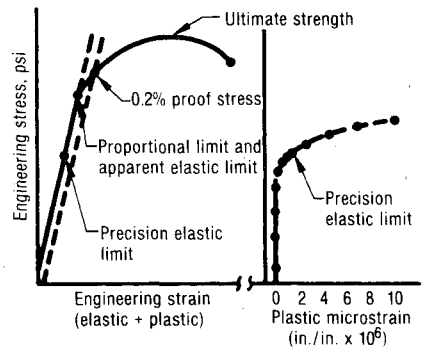

Fig. 1 Typical stress-strain curve.

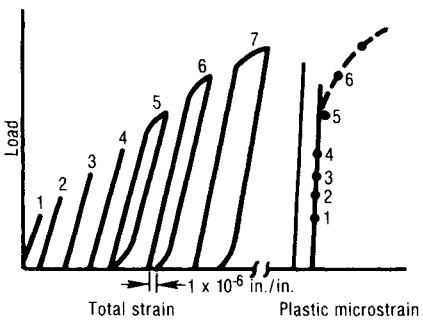

Fig. 2 Typical PEL determination.

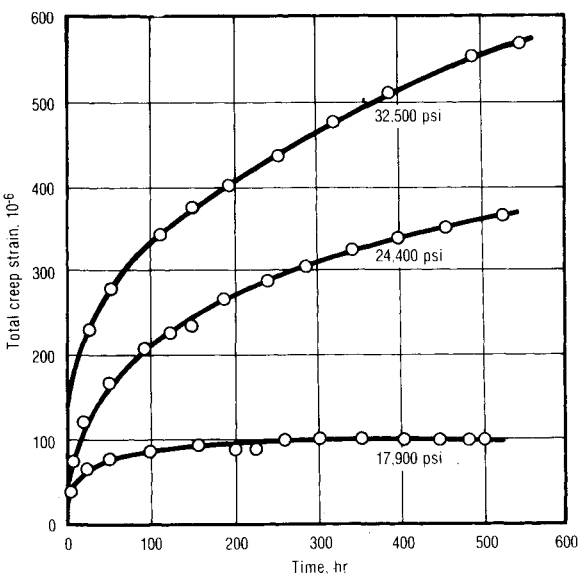

Fig. 3 Total creep curves of 310 stainless steel at 85°F.

stress. To avoid this metal problem, the metal stress must be completely relieved and use-application conditions must be reduced to less than the PEL stress value.

Typical differences between ultimate strength and PEL are shown in Table 1. Some materials experience very little difference, but other metals, such as 310 stainless steel, indicate a PEL stress of one-tenth the ultimate strength. Using 310 stainless steel as a reference and scaling the difference between ultimate strength the PEL of 15-5 stainless steel material yields a value of approximately 20,000 psi. Working below half this stress value (10,000 psi) should maintain metal stability over the desired 10-yr lifetime in rocket motor applications.

The complete stress-relief metal conditioning process is an item of major importance. The current transducer (machined from 15-5 stainless steel) has some parts electron-beam welded together and then subjected to the stress-relief metal conditioning process outlined in Table 2. The heating and cooling rates for annealing, cold soak, and 900°F precipitation heat treatment are all critical items selected for this particular transducer design.

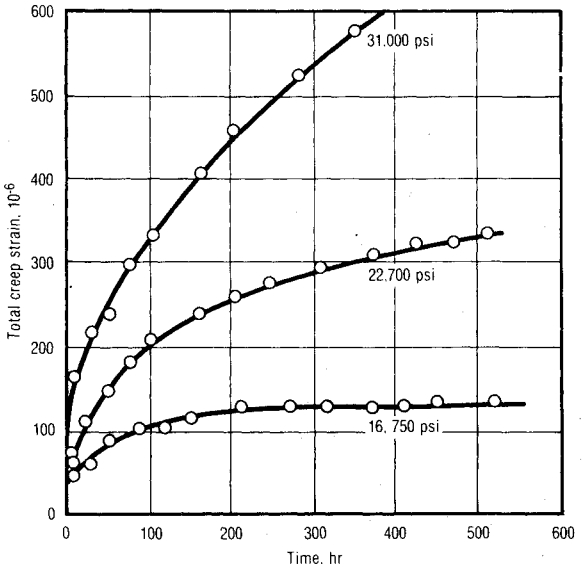

Fig. 4 Total creep curves of 310 stainless steel at 150°F.

Table 1 Precision elastic limit comparative chart

Material	Precision elastic limit, psi	Ultimate strength, psi
High-purity alumina	23,000	23,000
High-purity beryllia (ceramic)	20,000	20,000
Glass-bonded mica	4,000	9,000
Hot-pressed beryllium	2,000	45,000
AZ-31B magnesium rod	6,000	34,000
A356-T6 aluminum casting	12,000	40,000
2024-T6 aluminum extrusions	25,000	58,000
6AL-4V titanium rod, an.	70,000	150,000
310 CRES steel rod, CR and SR	11,000	120,000
Tool steel, high speed	50,000	180,000
Inconel-X	65,000	150,000

Table 2 Metal conditioning process[a]

Heat treat to 1900° ±25°F in argon atmosphere for ½ hour: cool from 1900° to 800°F in 15 ± 10 min and then cool to 70°F in the same length of time.

Cold soak samples to −100°F for 1 hr within 24 hr after air cooling to 70°F. Place hardware in bucket or other container in −100°F solution; this will prevent excessive thermal stresses exceeding the precision elastic limit during cooldown process. The 15-5 alloy is martensite at 70°F but may have minute amounts of metastable austenate. Dropping to −100°F or lower assures complete transformation to martensite. Air warm samples to 70°F at a rate of 100°F/hr or less.

Precipitation harden material at 900° ±25°F for 1 hr; air cool to 70°F at a rate of 100°F/hr or less.

Descale hardware with grit blast procedure to remove discoloration (oxidation).

[a] Metal conditioning process conducted after all transducer metal parts are machined.

Diaphragm Strain Gage Selection

An optimum design would have the semiconductor strain gages and metal housing sized such that both tension and compression gages have the same strain values. Finite-element structural analysis was conducted to define the integrated

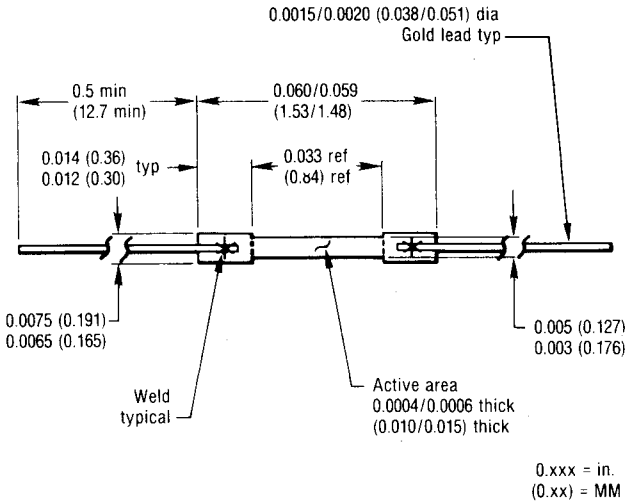

Fig. 5 Selected semiconductor strain gage.

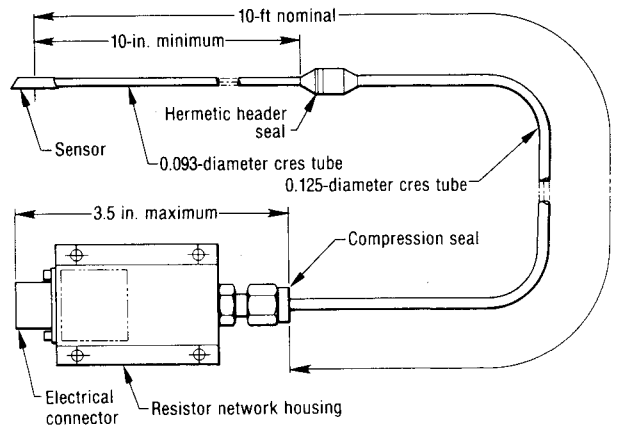

Fig. 6 Low-profile stress transducer assembly.

average strain across the gages for 0.040, 0.060, and 0.080 in. semiconductor strain gages. The 0.060 in. gage was selected because the diaphragm central and outside strains were more closely matched. This will maximize electrical output and contribute to gage stability. Details of the selected strain gage are presented in Fig. 5.

Miniature Stress Transducer Design and Fabrication Procedures

The final transducer design is presented in Figs. 6 and 7 and has the following features:

1) All seals and seams are electron-beam welded except for the lead wire exits for which a glass-to-metal header is used.

2) The transducer body is fabricated with 15-5 SS to avoid directionality in metal properties and to eliminate metal occlusions.

3) The transducer structural design is optimized for stiffness and minimal stress disturbance and interaction with solid propellant.

4) Four semiconductor strain gages are used with 0.060 in. length for optimal electrical output and strain matching.

5) A glass-to-metal header is located remote from the transducer body to allow reduced transducer height and minimize electron beam welding heat on main sensor body.

6) Bridge completion and temperature compensation resistors have 5 ppm/°C-TC and 0.003%/yr stability and are remotely located to avoid fabrication heat and toxic chemical environment.

7) The semiconductor epoxy adhesive is filtered and processed to provide a bond thickness of 0.0005 in.[5]

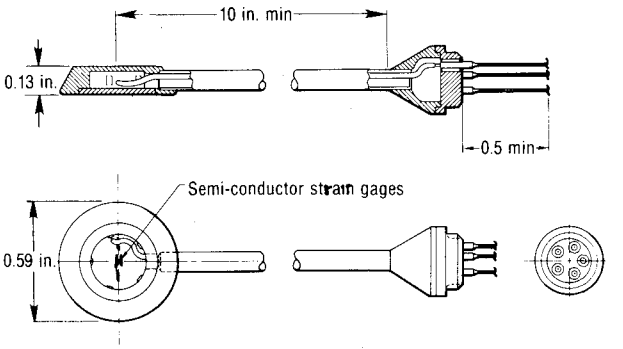

Fig. 7 Stress transducer design detail.

8) The stress gage metal bonding surface is finished to a roughness of 22 μ in.

9) Excitation is a 5 mA constant current to avoid field contact resistance changes and minimize transducer self heating problem.

A major design and fabrication goal is to achieve very stable transducer zero offset and sensitivity. Once this type of transducer is installed within a rocket motor it cannot be removed for further electrical calibration.

The zero offset variations are the most important since experience[6,7] has shown that transducer sensitivity does not change appreciably with time whereas zero offset data may drift with age.

One parameter affecting zero offset stability is the condition of the metal after the transducer is manufactured. Literature surveys and metallurgy studies have shown that 15-5 stainless steel is the best material for corrosion resistance, long-time stability, and uniformity of properties.[3,4] The 15-5 stainless steel goes through a double vacuum melt to eliminate metal occlusions and directionality in properties and has chemical corrosion resistance equivalent to or better than 17-4 stainless steel. Since 15-5 PH has fewer and smaller occulsions due to a double vacuum melting process there is less probability of obtaining a transducer which has a metal occulsion in the thin diaphragm or other structural member of the transducer.

Proper processing and curing of the epoxy used to bond the semiconductor strain gage to the metal diaphragm was necessary to reduce the thermally induced stresses in the bond system. A thermal step-cure process was chosen to reduce the stresses in the bond system when the transducer is cooled to normal application temperatures. Cure was initiated at 160°F and then increased in a step-wise fashion to obtain complete cure at a minimum average temperature. Epoxy thickness was controlled at approximately 0.0005 in. by filtering the epoxy, controlling metal roughness, and special processing.

The net result of the metal conditioning process and epoxy application procedures is to reduce the "built-in" metal and epoxy thermal stresses that contribute to transducer instability.

Passive Temperature Compensation

Passive temperature compensation of semiconductor strain gage bridges has been effectively used for over ten years and has several important advantages. Compensation is achieved by series or shunt low TC resistors. Since these resistors do not need to see the temperature to effect compensation they can be located internal or external to the transducer and their thermal time constants have no effect on the transducer. This leaves the strain gage as the only active compensating agent thereby minimizing transient errors.

Testing at low output signals and low operating strain levels has shown that the stability of the stress gage is limited by the RN55C metal film resistor used in effecting the temperature compensation and bridge completion. These resistors have a 50 ppm/°C-TC and small thermal variations cause detectable

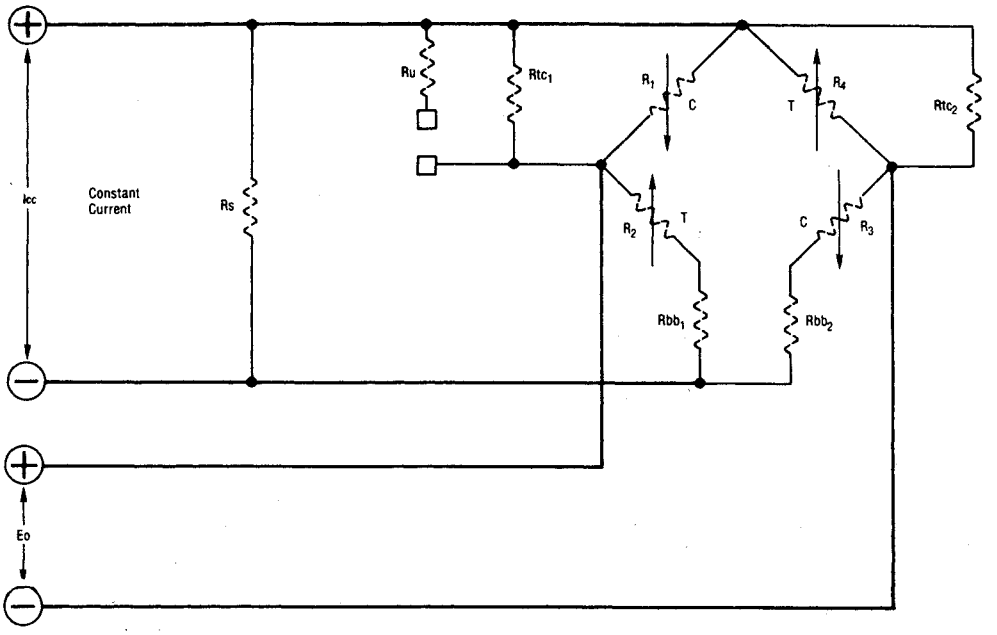

Fig. 8 Fully active semiconductor strain gage bridge with passive temperature compensation.

Table 3 Transducer performance characteristics

	Senso-Metrics data[a]			CSD data[b]					
Transducer	FS OP, mV	Se, mV/psi	Linearity, hysteresis, repeatability, %FS	FS OP, mV	Se, mV/psi	Linearity, % FS	Hysteresis, % FS	Repeatability % FS	Precision index, % FS
B381	9.09	0.364	0.44						
B382	8.15	0.326	0.12						
B383	7.66	0.306	0.26	7.74	0.310	0.189	0.295	0.229	0.123
B384	8.60	0.344	0.12						
B385	7.05	0.282	0.14						
B386	7.37	0.295	0.28						
B387	8.49	0.340	0.16	8.44	0.337	0.149	0.212	0.130	0.116
B388	8.23	0.329	0.12						
B390	7.78	0.311	0.12	7.85	0.314	0.152	0.253	0.053	0.122
B392	6.97	0.279	0.30						
B396	7.20	0.288	0.14						
B389	243.54	0.122	0.22						
B394	234.60	0.117	0.76						
B395	227.74	0.114	0.80						

[a] Senso-Metrics data was measured in May 1978 at their facility before delivery to CSD. [b] CSD data was measured in June 1979 using an AMETEK dead weight calibration device; Model RK; demonstrator unit.

signal variations. Long-time stability of the RN55C was shown to be unacceptable for this transducer application.

The passive resistors used on this program have high stability (0.003%/yr) and 5 ppm/°C-TC or better to eliminate thermal transient effects. The Wheatstone bridge circuit with passive temperature compensation resistors is presented in Fig. 8 for the constant current excitation used with the stress transducer.

Transducer Performance

Fourteen transducers were fabricated and tested to evaluate performance characteristics of these miniature all-metal sealed units. Some of the primary data for these units is presented in Table 3. During data analysis of the 33-point pressure calibrations a statistical evaluation of linearity, hysteresis, repeatability, and precision index is conducted. Table 4 presents such an evaluation for transducer S/N B383.

The low-range (25 psi) transducers have stiff diaphragms to minimize the solid propellant interaction which accounts for their low full-scale output. These units would normally have been rated as 500-psi units for other applications. The combined transducer errors are very low magnitude for the low range transducer especially since its full scale output has been reduced for additional stiffness.

Stability Evaluation

Several of these transducers were subjected to long-term stability testing in the laboratory. This consisted of measuring the zero offset periodically while the transducer was stored at 70°F. Since this transducer is a 25-psi absolute unit, the long time storage condition is over half scale load at 14.7 psi. The transducers were also pressure calibrated a few times and cycled between −65°F and 160°F once or more.

Transducer Offset Stability

Zero offset and calibration measurements were made with the equipment illustrated in Fig. 9. Zero offsets were obtained with the transducer removed from the pressure vessel. The precise constant current value is determined from the voltage drop across a precision ten ohm resistor. The resistor is a low TC resistor (1 ppm TC) and has 0.1% accuracy and 0.003%/yr stability. Barometric pressure was recorded with a

Table 4 Statistical evaluation

% FS pressure		0%	20%	40%	60%	80%	100%
NOP (sensitivity curve)	mV	=3.989	5.537	7.086	8.634	10.182	11.730
Linearity	mV	=0.005	0.015	0.015	0.011	0.010	0.005
	% FS OP	=0.060	0.190	0.189	0.144	0.132	0.069
Hysteresis							
Run 1	mV	=0.002	0.004	0.003	0.012	0.012	0.000
	% FS OP	=0.025	0.050	0.044	0.151	0.159	0.000
Run 2	mV	=0.002	0.003	0.016	0.014	0.020	0.000
	% FS OP	=0.024	0.036	0.203	0.179	0.254	0.000
Run 3	mV	=0.001	0.009	0.023	0.019	0.017	0.000
	% FS OP	=0.013	0.115	0.295	0.246	0.218	0.000
Repeatability							
Increasing	mV	=0.002	0.017	0.018	0.004	0.007	0.008
	% FS OP	=0.030	0.215	0.229	0.055	0.088	0.100
Decreasing	mV	=0.001	0.004	0.002	0.004	0.001	0.008
	% FS OP	=0.018	0.050	0.022	0.051	0.007	0.100
Precision index	mV	=0.004	0.009	0.010	0.009	0.009	0.005
	% FS OP	=0.051	0.110	0.123	0.110	0.121	0.070

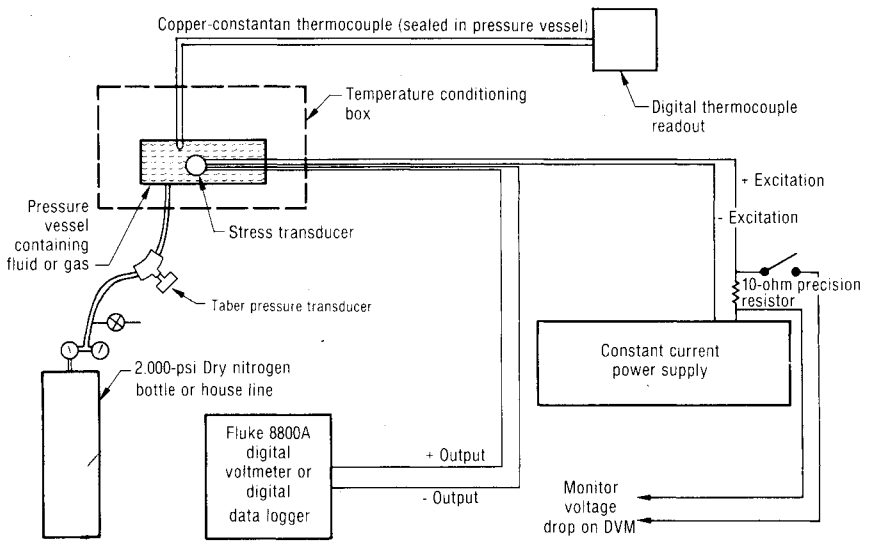

Fig. 9 Stress transducer calibration and data acquisition system.

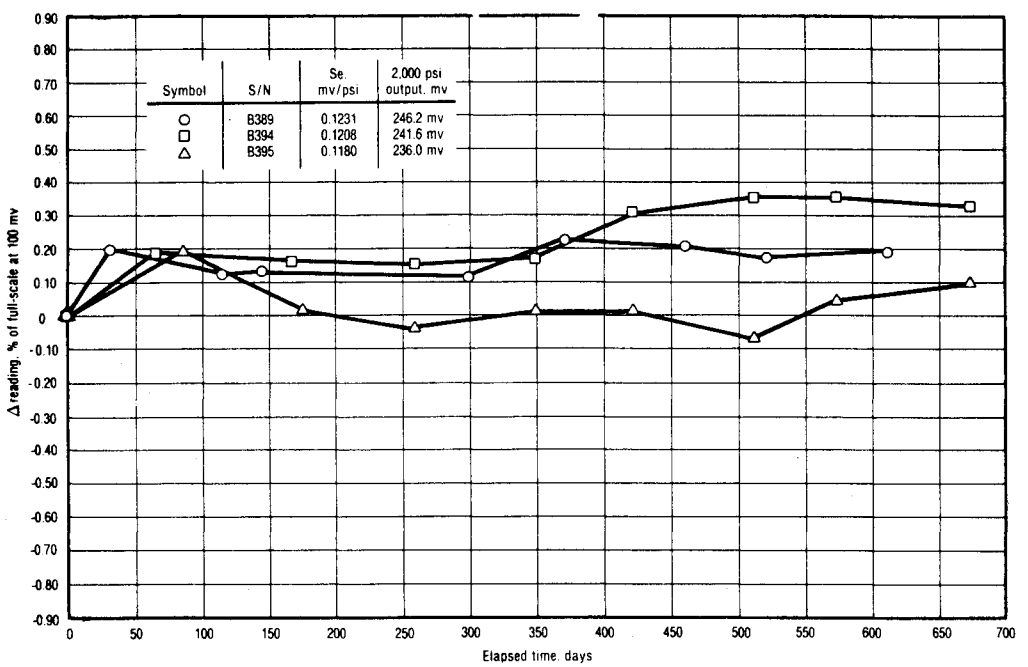

Fig. 10 14.7 psi offset history for 2000 psi Senso-Metrics Stress Transducer (Model 601156).

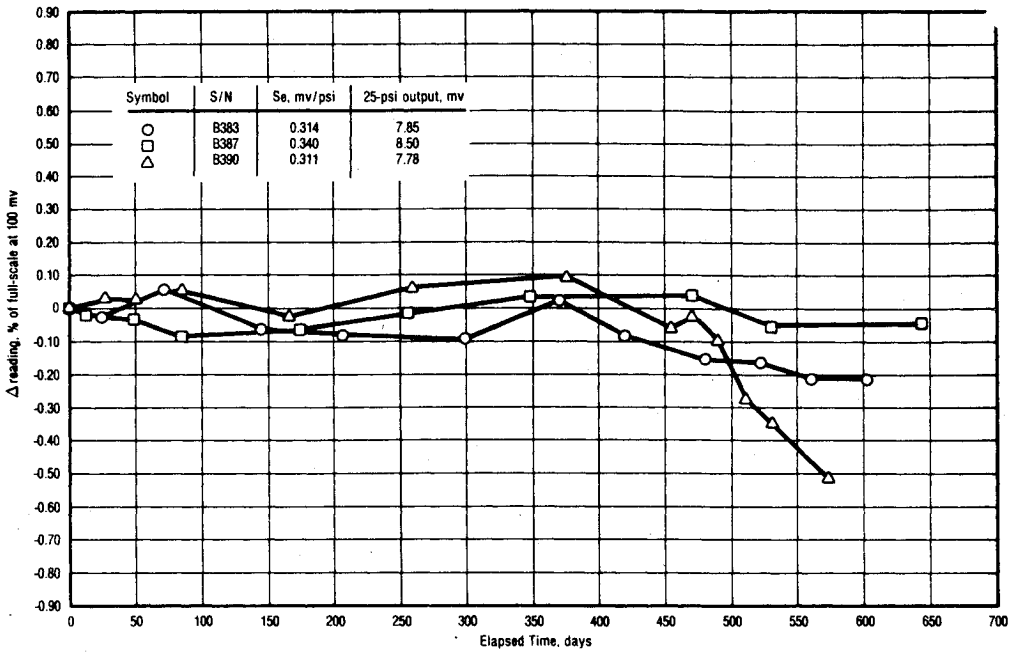

Fig. 11 14.7 psi offset history for 25 psi Senso-Metrics Stress Transducers.

Wallace-Tiernan pressure meter, Model FA129 (0-20 psi with 0.02 psi resolution). All data was recorded and maintained on an HP-9825 computer storage system for further data analysis and graphing.

The 14.7 psi offset, ZO_c, corrected for barometric pressure and current variation is used to determine the stability of the transducer. The ΔZO_c is the 14.7 psi output voltage change and $\%ZO_c$ is related to the measured full-scale output. The final corrected no-load output for each transducer is plotted vs aging time to show aging trends. Figures 10 and 11 present long term zero offset data for several production gages of both 25-psi and 2000-psi ranges. None of these transducers vary more than approximately 0.5% at a nominal 100 mV output over the testing time. The largest change in the 14.7 psi offset values occurred after pressure calibrations and generally returned to normal within a reasonable time.

Stress Disturbance, Interaction, and Nonuniform Stress Field

Three physical factors are required in data interpretation for the transducer when embedded in the nonlinear viscoelastic solid propellant.

1) Stress disturbance—The propellant stress being measured is altered by the stress transducer.

2) Transducer-propellant interaction—The diaphragm stiffness is affected by the rigidity of the solid propellant.

3) Nonuniform stress field—The solid propellant bond stress being measured may not be uniform in the location of the desired stress measurement.

The change in propellant stress at the diaphragm/propellant interface is caused by the inclusion of the metal structure and the flexure of the metal diaphragm. This effect includes the stress disturbance and a propellant-modulus interaction of the transducer. This propellant interaction is caused by the propellant providing some structural support for the diaphragm. Transducer design goals were to minimize this interaction by making the diaphragm thicker, but the final thickness was based on a trade-off between electrical output and propellant-transducer interaction factor.

The transducer subjected to a load while embedded in propellant undergoes diaphragm deformation that is different from that induced by a hydrostatic pressure during calibration. This transducer-propellant interaction was considered using structural analysis of the test model with and without the transducer.[8] The radial strain for the transducer diaphragm (and therefore strain gages) are computer calculated. The absolute value of the average integrated radial strains was used to determine the transducer-propellant correction factors.

Table 5 Correction factors for Senso-Metrics 2000-psi transducer

	Thermal load	Gravity load	Pressure load
I_f, transducer interaction factor	0.997	0.990	0.996
D_f, transducer disturbance factor	1.08	0.994	0.995

$$\text{Propellant stress } (\sigma) = \frac{\text{transducer output-zero offset}}{\text{sensitivity}} (I_f)(D_f)(N_f)$$

where I_f is the interaction factor from finite-element analysis (range: 0%-2%), D_f is the stress disturbance factor from finite-element analysis (range: 0%-20%), and N_f is the nonuniform stress field factor from finite-element analysis (range: 0%-5%).

These factors are a function of the solid propellant modulus and specific motor application condition. Specific structural analysis correction factors for the Senso-Metrics 2000-psi transducer in an end-burner fixture with a propellant modulus of 500 psi are given in Table 5.

Analysis of solid propellant stress transducer application conditions shows that each transducer will have a specific stress disturbance and interaction effect depending on the geometry of the vehicle in which it is mounted. These effects can be readily determined for any thermal or pressure loading condition using finite element analysis techniques.

Conclusions

A summary of the main conclusions follows:

1) A stress transducer increasing the state-of-the-art in solid propellant stress measurement was designed, manufactured, and evaluated. This transducer uses new design concepts, fabrication procedures, evaluation techniques, and analytic considerations.

2) Finite-element analysis results were used successfully to optimize the gage geometry, to minimize propellant stress disturbance, and to convert from the electrical measurements to meaningful stress values.

3) Chemical protection from the corrosive solid propellant environment was achieved by using electron-beam welded seals and a glass-to-metal header for wire exits.

4) Metal stability was achieved by selecting 15-5 stainless steel and using an elaborate metal conditioning-stabilization process after transducer fabrication to insure that stresses do not exceed the precision elastic limit.

5) Transducer stability was further improved by reducing epoxy thickness to approximately 0.0005 in., filtering out large particles in epoxy, and step curing with final temperature of 350°F.

6) Constant current excitation was selected to provide improved safety, compensation, and application advantages.

This new transducer design is a significant improvement over other conventional transducers previously considered for use in solid propellant rocket motors.

References

[1] Francis, E.C. and Briggs, W.E., "Use of Structural Analysis In Optimum Design of Improved Stress Transducers," 23rd International Instrumentation Symposium, Instrument Society of America, Las Vegas, Nev., May 1977.

[2] Francis, E.C. and Thompson, R.E., "Solid Propellant Stress Transducer Evaluation," 24th International Instrumentation Symposium, Instrument Society of America, Albuquerque, N. Mex., 1978.

[3] Francis, E.C., Thompson, R.E., and Briggs, W.E., "The Development of Improved Normal Stress Transducer for Propellant Grains," CSD 2548-FR, June 1979, Chemical Systems Divison of United Technologies, Sunnyvale, Calif., AFRPL-TR-79-34.

[4] Maringer, R.E., Glaeser, W.A., and Olofson, C.T., "Material Properties Pertinent to the ISUS Sensor Block," Battelle Memorial Institute, Columbus Laboratories, April 9, 1980.

[5] Chew, T.J. and Banasiak, D.H., "A Microphotographic Study of an Epoxy Bond System For Semi-Conductor Stress Transducers," Air Force Rocket Propulsion Laboratory, Edwards AFB, Calif., AFRPL-TR-77-39, Aug. 1977.

[6] Leder, P.S., "Life Cycling Test on Several Strain Gage Pressure Transducers," *NBS Technical Note 434,* Oct. 1967.

[7] Williams, R., "The Effects of Extended High-Temperature Storage on the Performance Characteristics of Several Strain Gage Pressure Transducers," *NBS Technical Note 497,* Oct. 1969.

[8] Francis, E.C. and Briggs, W.E., "Solid Propellant Stress Transducer Considerations," 26th International Instrumentation Symposium, Instrument Society of America, Seattle, Washington, May 1980.